2014 International Conference on Mechatronics and Control (ICMC)
July 3 - 5, 2014, Jinzhou, China

Evaluation of an Analytic Model for Car Dynamics

M. Ruf*†, J. R. Ziehn*‡§, D. Willersinn*, B. Rosenhahn‡, J. Beyerer*† and H. Gotzig¶

*Fraunhofer Institute of Optronics, System Technologies and Image Exploitation (IOSB), 76131 Karlsruhe, Germany
Email: {miriam.ruf, jens.ziehn, dieter.willersinn, juergen.beyerer}@iosb.fraunhofer.de

†Vision and Fusion Laboratory (IES), Karlsruhe Institute of Technology (KIT), 76131 Karlsruhe, Germany
Email: miriam.ruf@kit.edu

‡Institut für Informationsverarbeitung (TNT), Leibniz Universität Hannover, 30167 Hanover, Germany
Email: {rosenhahn, ziehn}@tnt.uni-hannover.de

¶Valeo Schalter und Sensoren GmbH, 74321 Bietigheim-Bissingen, Germany
Email: heinrich.gotzig@valeo.com

***Abstract*—This paper presents and evaluates a differential geometric model for single and double track vehicles, which allows to estimate internal state parameters (steering angles, velocities, wheel speeds, ...) from a given planar trajectory over time. Possible applications include accident reconstruction from video footage, constraining trajectory optimization by physical limits, and extracting control parameters a-priori from trajectories, for use in open-loop (non-feedback) controllers for short intervals. The model is easy to compute, yet the evaluation with IPG CarMaker suggests a good level of accuracy.**

I. Introduction

Vehicle models are applied in driver assistance systems to make the behavior of the ego vehicle computable using simplifying assumptions to a certain degree. Commonly these models are based on differential equations that allow to predict the vehicle behavior based on the control inputs.

The model presented here for evaluation is a (single or double track) model with a focus on easy computation based on differential geometry properties of the given trajectory, assuming it is twice continuously differentiable (hence the name C^2 model). Applications include deriving the control commands from a pre-computed trajectory, or supporting the computation of a physically feasible trajectory (e.g. by variational methods, [10]) by providing a simple way of imposing hard constraints on control inputs, such as steering angles and angular velocities, or vehicle speeds and accelerations. The applicability of the model for both purposes will be evaluated in this paper.

II. State of the Art

Depending on the desired level of detail and the system information available, there exist different approaches for modeling vehicle dynamics [5], which can be used for predicting the behavior—and therefore the future trajectory—of an ego vehicle. The most common method to plan this trajectory is to use differential equations to model the influence of the control parameters on the vehicle state ([7], [1], [4], [6]), and thereby predict the trajectory given a set of control parameters. This approach is advantageous for assuring that only valid control parameters are used in optimization, and—depending on the vehicle model—it can be very accurate. Yet, the computational effort is high and modeling can be difficult because trajectory planning is performed by manipulating the inputs, not the trajectory itself. To limit the computational effort, simplified models of vehicle dynamics are used.

To the knowledge of the authors, thus far no detailed model for analyzing a positional trajectory for state and control parameters has been presented and evaluated for automotive applications.

§Corresponding author

III. Model Derivation

In this section the presented model will be motivated and derived geometrically.

A. Vehicle Model

The vehicle model in this paper can be a single track or double track model. The following vehicle parameters are utilized in the model:

- The *wheel base* l, which is the distance between the front and the rear axle.
- The *half width* h of the track, which is half the distance between wheels on the same axle.
- The *tire radii* r^{front} and r^{rear} at the respective axes.

The vehicle state is taken to be comprised entirely of

- its *position* $\boldsymbol{\xi} = [\xi_{\text{x}}, \xi_{\text{y}}]^{\mathsf{T}}$, which is taken to lie on the center of the rear axle (cf. Fig. 1),
- its *velocity* $\mathrm{d}\boldsymbol{\xi}/\mathrm{d}t = \dot{\boldsymbol{\xi}} = [\dot{\xi}_{\text{x}}, \dot{\xi}_{\text{y}}]^{\mathsf{T}}$, which always points into the heading direction ψ,
- its *steering wheel angle* δ^{w}, which maps to the left and right *tire angles* $\delta^{\text{left}}, \delta^{\text{right}}$, and to the *mean tire angle* $\delta = (\delta^{\text{left}} + \delta^{\text{right}})/2$, and
- its *tire rotation angles* around the car axes, for the front left, front right, rear left and rear right tires $\rho^{\text{fl}}, \rho^{\text{fr}}, \rho^{\text{rl}}, \rho^{\text{rr}}$.

Notable simplifications, some of which are incorporated in the single track model [8], include:

- The tire slip is assumed to be zero at all tires at all times, both for lateral and longitudinal slip.

978-1-4799-2537-7/14/$31.00 ©2014 IEEE

- Bank (roll) and pitch angles of the vehicle are not considered.
- The vertical axis is not considered; the center of gravity lies in the 2D plane.
- Wheel loads and varying radii are not considered.
- Any internal structure, such as engine and gears, is omitted. (For vehicle control, a drive-by-wire system is assumed to be in place that operates based on desired steering wheel angles δ^{w} and accelerations a.)

B. Trajectories

A trajectory is taken to be the planar curve described by a car's *reference point*, which lies on the center of the rear axle (Fig. 1). This planar curve is defined by

$$\boldsymbol{\xi} \,:\, T \to X \times Y \tag{1}$$

where T is an interval of time, and X and Y represent Cartesian coordinates on the surface on which the ego vehicle can navigate. Further, $\boldsymbol{\xi}$ must lie in C^2 (i.e. be twice continuously differentiable), to assure that all parameters established here are well defined. If the surface has a non-Cartesian parametrization (for example due to curvature), the model derived in this section is invalid and Riemannian geometry must be applied [9, p. 127ff.], which is beyond the scope of this paper. However, it is assumed that taking the trajectory to lie on a Euclidean plane represents a suitable simplification for a wide range of practical applications.

C. State and Control Parameters

Derivatives of the trajectory will be denoted $\dot{\boldsymbol{\xi}} = \mathrm{d}\boldsymbol{\xi}/\mathrm{d}t$ and $\ddot{\boldsymbol{\xi}} = \mathrm{d}^2\boldsymbol{\xi}/(\mathrm{d}t)^2$. For any point along the trajectory, there is a base of $\mathbb{R}^2$ consisting of a tangent vector and a normal vector [3, p. 19]

$$\boldsymbol{T} = \frac{\dot{\boldsymbol{\xi}}}{\|\dot{\boldsymbol{\xi}}\|} \qquad \text{and} \qquad \boldsymbol{N} = \begin{bmatrix} 0 & -1 \\ 1 & 0 \end{bmatrix} \boldsymbol{T}. \tag{2}$$

The tangent vector must be continuous for the curvature (required later, in (5)) to be finite. Where $\boldsymbol{T}$ cannot be directly computed via (2), because $\dot{\boldsymbol{\xi}}(t) \equiv \boldsymbol{0}$ on any interval I, its value on I can be set to either of the outer limits for $\boldsymbol{T}$ on I. These limits should be identical, otherwise again the curvature will be infinite. If such limits exist for no choice of I, then the car is stationary ($\dot{\boldsymbol{\xi}}(t) \equiv \boldsymbol{0}$ for all t) and no directional parameters can be derived.

If the car's coordinate system is identified with the $(\boldsymbol{T}, \boldsymbol{N})$ base, the longitudinal speed and acceleration can thus be obtained as the projection of total velocities and accelerations onto the tangential vector:

$$v = \left\langle \boldsymbol{T} \,\middle|\, \dot{\boldsymbol{\xi}} \right\rangle = \frac{\left\langle \dot{\boldsymbol{\xi}} \,\middle|\, \dot{\boldsymbol{\xi}} \right\rangle}{\|\dot{\boldsymbol{\xi}}\|} = \|\dot{\boldsymbol{\xi}}\| \quad \text{and} \tag{3}$$

$$a = \left\langle \boldsymbol{T} \,\middle|\, \ddot{\boldsymbol{\xi}} \right\rangle = \frac{\left\langle \dot{\boldsymbol{\xi}} \,\middle|\, \ddot{\boldsymbol{\xi}} \right\rangle}{\|\dot{\boldsymbol{\xi}}\|}, \tag{4}$$

where the identification of bases makes use of the assumption that the slip be zero (i.e. $\langle \boldsymbol{N} | \dot{\boldsymbol{\xi}} \rangle \equiv 0$ at all times). It should also be noted that (4) is not $\|\ddot{\boldsymbol{\xi}}\|$ unless the vehicle is moving straight ahead.

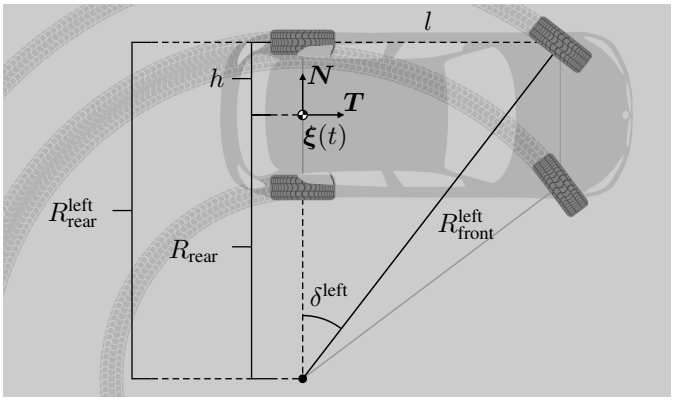

Fig. 1: Ackermann steering geometry in a constant curvature turn. The individual trajectories of every point on the car are concentric circles or varying radii. All tires are aligned tangential to their respective circles. The steering angles δ^{w} and δ^s effect the turn radius R_{rear} of the car's reference point along $\boldsymbol{\xi}$. In a right turn, $R_{\text{rear}} < 0$, so $R^{\text{left}}_{\text{rear}} = R_{\text{rear}} - h$ produces a larger absolute radius.

The curvature is defined (for arc length s; [2], [3]) by

$$\kappa = \left\langle \tfrac{\mathrm{d}}{\mathrm{d}s}\boldsymbol{T} \,\middle|\, \boldsymbol{N} \right\rangle = \frac{\det[\dot{\boldsymbol{T}}, \boldsymbol{T}]}{\|\dot{\boldsymbol{\xi}}\|} = \frac{\det[\dot{\boldsymbol{T}}, \dot{\boldsymbol{\xi}}]}{\|\dot{\boldsymbol{\xi}}\|^2} = \frac{\det[\ddot{\boldsymbol{\xi}}, \dot{\boldsymbol{\xi}}]}{\|\dot{\boldsymbol{\xi}}\|^3} \tag{5}$$

and specifies the circular approximation of the trajectory at every point: The circle that approximates $\boldsymbol{\xi}$ lies in the direction of $\boldsymbol{N}$ off the trajectory at a distance and radius of $\kappa^{-1} = R_{\text{rear}}$, the turn radius of the ego vehicle's reference point (cf. Fig. 1) (not to be confused with the rear tire radius, r_{rear}). Both curvature and radius are negative for right turns (see Fig. 1).

The turn radius of the car is effected by the front tire angles, δ^s, with $s \in \{\text{left}, \text{right}\}$, and (indirectly) the steering wheel angle δ^{w}. Figure 1 shows the geometry that is used to derive the front left tire angle δ^{left} from the rear axle turn radius R_{rear} (described by the trajectory $\boldsymbol{\xi}$). Since all four tires describe concentric turn circles (albeit at four different radii R^s_{rear} and R^s_{front}), and since their direction of motion is tangential to their respective circles, the right triangle in Fig. 1 can be established. The effect of the front tire angle δ^s on the rear tire turn radius R^s_{rear} is mediated by the wheel base l and the half track width h via:

$$\begin{array}{lll} \delta^s = \arctan\left(\dfrac{l}{R^s_{\text{rear}}}\right) & & = \arctan\left(l\,\kappa^s\right) \\ \quad\Big| & & \quad\Big| \\ \quad = \arctan\left(\dfrac{l}{R_{\text{rear}} \pm^s h}\right) & & = \arctan\left(l\,\kappa\,\dfrac{R_{\text{rear}}}{R^s_{\text{rear}}}\right) \end{array} \tag{6}$$

(where κ^s is the curvature of the individual front tire trajectories, and $\pm^{\text{left}} = -, \pm^{\text{right}} = +$) using the curvature calculated in (5). It should be noted that the use of $\mathrm{atan2}$ is not necessary here since the tire angles are certainly limited to $\pm\pi/2$.

Using the tire radii r_{front} and r_{rear}, the angular velocities of the tires can be obtained as

$$\dot{\rho}^{\mathrm{r}s} = \frac{\|\dot{\boldsymbol{\xi}}\|}{r_{\text{rear}}} \cdot \frac{R^s_{\text{rear}}}{R_{\text{rear}}} = \frac{\|\dot{\boldsymbol{\xi}}\|}{r_{\text{rear}}} \cdot \frac{R_{\text{rear}} \pm^s h}{R_{\text{rear}}} \tag{7}$$

and

$$\dot{\rho}^{\mathrm{f}s} = \frac{\|\dot{\boldsymbol{\xi}}\|}{r_{\text{front}}} \cdot \frac{R^s_{\text{front}}}{R_{\text{rear}}} = \frac{\|\dot{\boldsymbol{\xi}}\|}{r_{\text{front}}} \cdot \frac{\sqrt{l^2 + (R_{\text{rear}} \pm^s h)^2}}{R_{\text{rear}}}. \tag{8}$$

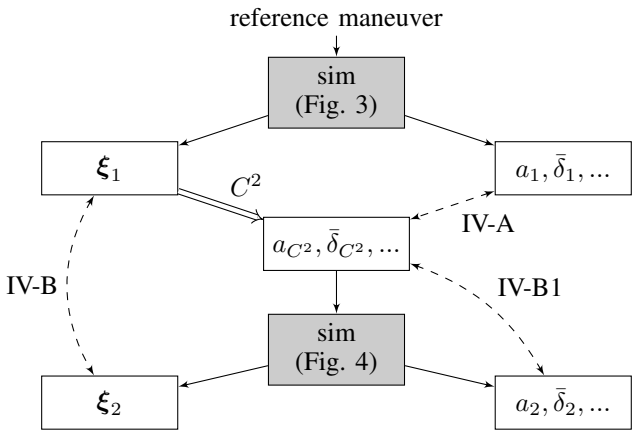

Fig. 2: Structure of the evaluation of the C^2 model: A reference maneuver is passed to CarMaker for simulation. The simulation yields a trajectory $\boldsymbol{\xi}_1$ and internal parameters a_1, $\bar{\delta}_1$, etc. The trajectory is passed to the C^2 model. The resulting estimated parameters are compared directly in Figs. 9 and 10. Accelerations and steering wheel angles are further used as control inputs to another simulation, which again yields a trajectory $\boldsymbol{\xi}_2$ and internal parameters a_2, $\bar{\delta}_2$, etc. The obtained results are discussed in the sections indicated by dashed arrows.

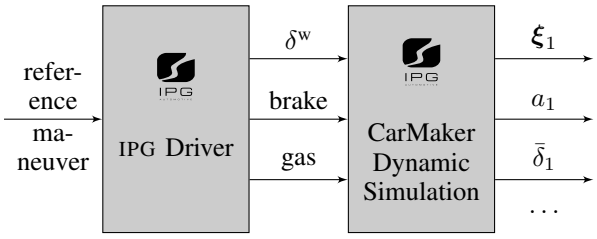

Fig. 3: Structure of the first simulation from Fig. 2. A given reference maneuver is passed to the CarMaker "Driver" subsystem, which finds control parameters δ^{w}, brake and gas to execute the reference maneuver as closely as possible. These inputs are then passed to the CarMaker Dynamic Simulation of the actual car, yielding the outputs described in Fig. 2.

The heading direction ψ, or yaw, can be specified relative to a "north" direction $\boldsymbol{n}$ as

$$\psi = \measuredangle(\boldsymbol{T}, \boldsymbol{n}) = \measuredangle(\dot{\boldsymbol{\xi}}, \boldsymbol{n}) = \operatorname{atan2}\Big(\det[\boldsymbol{n}, \dot{\boldsymbol{\xi}}], \langle \boldsymbol{n} | \dot{\boldsymbol{\xi}} \rangle\Big), \quad (9)$$

and its derivative, the yaw rate, is thus

$$\dot{\psi} = \frac{\det[\ddot{\boldsymbol{\xi}}, \dot{\boldsymbol{\xi}}]}{\|\dot{\boldsymbol{\xi}}\|}. \quad (10)$$

IV. Model Evaluation

The properties defined above can be computed for every point along any twice continuously differentiable (non-static) trajectory. This allows to transform a surface curve into control and state parameters for a simple vehicle model. In this section, the model accuracy for two possible applications will be highlighted.

A. True Maneuver vs. C^2 model Analysis

This is arguably the most conclusive comparison. An observed trajectory $\boldsymbol{\xi}_1$ is analyzed by the C^2 model to estimate the state variables and control parameters that were attained during the maneuver. Common purposes of this step would be the following:

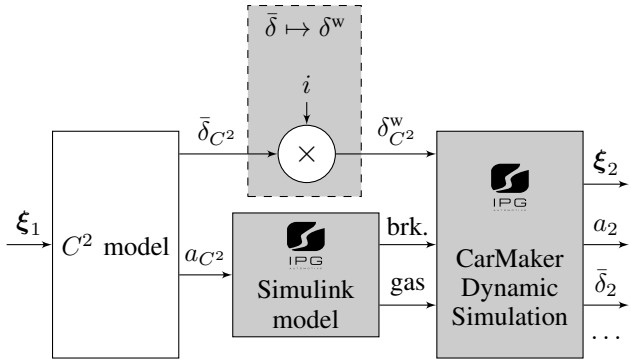

Fig. 4: Structure of the second simulation from Fig. 2. A given trajectory $\boldsymbol{\xi}_1$ is passed to the C^2 model to obtain parameters $a_{C^2}, \bar{\delta}_{C^2}$. Desired accelerations a_{C^2} are passed to an IPG ACC model included in CarMaker, which finds control parameters brake and gas to achieve these accelerations. The mean tire angle $\bar{\delta}_{C^2}$ is turned into steering wheel angles $\delta^{\mathrm{w}}_{C^2}$ by a linear factor i, as a simplification. These inputs are then passed to the CarMaker Dynamic Simulation of the actual car, yielding the outputs described in Fig. 2.

- "Reverse-engineering" vehicle states from e.g. a video camera or on-board recording of positions.
- Constraining trajectory optimization processes to physically possible states.

In this evaluation, a BMW 118i is modeled in the simulation software IPG CarMaker. The simulation is performed at a rate of 1 000 Hz in CarMaker, the output values as passed on to the C^2 model and used in the evaluation are sampled at a rate of 100 Hz.

1) Sine Steering: To evaluate the robustness to steering, the simulated BMW drives at a constant goal speed of $v \in \{6\,\mathrm{km/h}, 30\,\mathrm{km/h}, 50\,\mathrm{km/h}\}$ and steers with a steering wheel angle of $\delta^{\mathrm{w}} = A \cdot \sin(2\pi t/\tau)$, $A \in [0, \pi]$, $t \in [0\,\mathrm{s},\ 40\,\mathrm{s}]$, $\tau \in [1\,\mathrm{s}, 20\,\mathrm{s}]$. The true state variables from CarMaker, $a_1, \delta^{\mathrm{w}}_1, ...$ are compared to the estimates from the C^2 model, $a_{C^2}, \delta^{\mathrm{w}}_{C^2}, ...$ using the error metric (for any state quantity x)

$$E_x = \sqrt{\frac{1}{40\,\mathrm{s}} \int_{t=0\,\mathrm{s}}^{40\,\mathrm{s}} \mathrm{d}t \, \Big(x_1(t) - x_{C^2}(t)\Big)^2}. \quad (11)$$

The error in Fig. 5b shows, that the mean tire angle accuracy deteriorates with increasing frequency and amplitude A of the steering wheel angle, as would be expected. The order of errors is approximately 0.2 rad, with the error increasing approximately linearly with frequency, and slightly superlinearly with the steering wheel angle.

Contrary to this, the errors in velocity (Fig. 5a) and acceleration show a salient pattern varying over the period length. This pattern correlates with the car's bank angle error and can be attributed to a violation of the models assumptions for the vehicle to remain level at all times. Remarkably the error decreases for some period lengths at increasing amplitudes, suggesting that parametrization errors, possibly in the tire radii, are counteracted by the errors due to bank angles.

2) Race Track: To evaluate the model in a realistic combination of various maneuvers, the simulation is applied to the *Hockenheimring* race track in Germany (a map can be found in Fig. 7, black line). The race track has a length of 4.574 km and is driven in the clockwise sense. In the first step, the

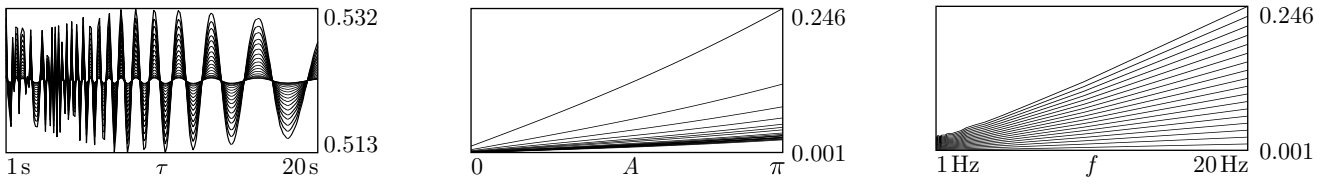

(a) E_v in [m/s] (b) E_δ in [rad] (c) E_δ in [rad]

Fig. 6: Errors as shown in Fig. 5, as families of curves. (c) is plotted over f instead of τ, to reveal the linearity.

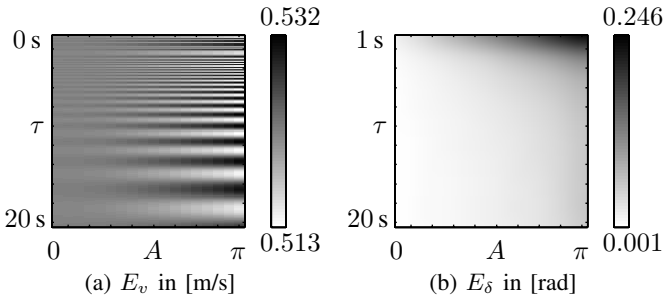

(a) E_v in [m/s] (b) E_δ in [rad]

Fig. 5: Errors obtained at the sine steering example (Sec. IV-A1) at $v = 50$ km/h.

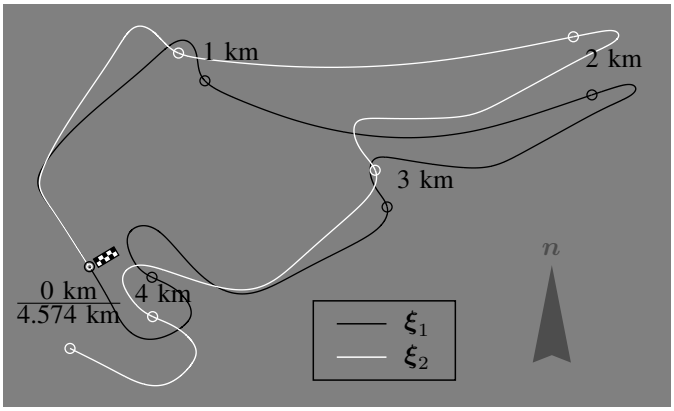

Fig. 7: Hockenheimring (true shape $\boldsymbol{\xi}_1$, black) traversed with an open-loop controller ($\boldsymbol{\xi}_2$, white) based only on precomputed steering angles and accelerations extracted from a normal traversal $\boldsymbol{\xi}_1$ via the C^2 model. The milestones (in kilometers) are shown as dots.

CarMaker module IPG Driver is used to automatically drive along the track at maximum speed; a top speed of 170 km/h is attained. The comparison of true parameters with the C^2 model estimates over the path length can be found in Fig. 10, the correlation between them is shown in Fig. 9. The latter states the mean error μ and the standard deviation σ of the error. It furthermore states the slope of the linear least squares approximation of the measurements, namely the pseudoinverse solution m to

$$x_1(t) \cdot m = x_{C^2}(t)$$

for any state quantity x over all measurement times t, which yields the m to minimize $\int \mathrm{d}t\,(x_1(t) \cdot m - x_{C^2}(t))^2$, consistently with (11). This m indicates a systematic factor between the estimated value x_{C^2} and the ground truth x_1.

The velocities (Fig. 9b) show an excellent correlation, the accelerations (Fig. 9a) deviate more notably, partly due to discretization. Figs. 9e and 9f show mostly a good correlation, but also the effects of the violated assumption of zero longitudinal slip: The small spikes to the left and right occur, when either the brake, or the gas pedal is pushed notably. The tire speed changes almost instantaneously (the BMW has a rear-wheel drive), while due to slip, the vehicle speed does not react without delay. During this delay the spikes of high deviation form, since the C^2 model cannot derive the change in wheel speed from the vehicle speed. The front wheels, which are not connected to the drivetrain, are not subject to these effects.

The tire steering angles (Fig. 9c–f) exhibit a slightly curved trend, which can stem from errors in wheel base l and half track width h.

Figure 10d shows an extract of the tire angle where $\bar{\delta}_{C^2}$ deviates notably from $\bar{\delta}_1$. The extract corresponds to the slight and elongated left bend between 1 km and 2 km (cf. Fig. 7). The C^2 model estimates a steering angle that would follow the bend at perfect grip. The simulated BMW however passes the bend in a drift/slip state, with a notable lateral speed $\langle \dot{\boldsymbol{\xi}} | \boldsymbol{N} \rangle \approx -3$ km/h, as shown in Fig. 10e (however at longitudinal speed $\langle \dot{\boldsymbol{\xi}} | \boldsymbol{T} \rangle \approx 170$ km/h), and is thus oversteering. Since lateral slip, and thus lateral speed is not considered in the C^2 model, the tire steering angle $\bar{\delta}_{C^2}$ is lower (due to a lack of oversteering).

B. C^2 Model Input vs. Execution of Results as Open-Loop Control Parameters

In this comparison, it is shown how a given trajectory $\boldsymbol{\xi}_1$ can be analyzed by the C^2 model to find control parameters $a_{C^2}, \delta^{\mathrm{w}}_{C^2}$ for an open-loop (non-feedback) controller. The resulting trajectory $\boldsymbol{\xi}_2$ is compared to the original $\boldsymbol{\xi}_1$.

The analysis in this step is less conclusive than the one in the previous Section IV-A, since a major factor is how well the ego vehicle (in this case the IPG ACC along with the assumption of a constant steering ratio $i \approx 18.4$) executes the control parameters a_{C^2} and $\delta^{\mathrm{w}}_{C^2}$. Therefore, this evaluation essentially demonstrates a lower bound of quality, which can be achieved by a very simple control model. More sophisticated models would likely be able to reproduce the desired parameters $a_{C^2}, \bar{\delta}_{C^2}$ much more closely (while still not using feedback). Figure 7 shows the positional deviation that would occur if the entire Hockenheimring is navigated via the offline control parameters $a_{C^2}, \delta^{\mathrm{w}}_{C^2}$ by an open-loop controller. Naturally, navigating approximately 5 km without feedback based on predetermined parameters is bound to produce a significant error, however the resemblance between $\boldsymbol{\xi}_1$ and $\boldsymbol{\xi}_2$ is notable. An evaluation that divided the Hockenheimring into increasingly small segments and measured the mean end point deviation per segment length converged towards an order of $3\,\mathrm{cm}/1\,\mathrm{m}$.

1) C^2 Model Output vs. Execution of Results as Open-Loop Control Parameters: Even though the comparison of the C^2 model outputs and the original control parameters of

$\boldsymbol{\xi}_1$ show promising results, the second simulation shows a significant offset, as discussed above. To convey an impression of how the deviations in the steering ratio and the drive-by-wire ACC used in the second simulation affect the quality of the results (compared to influences due to the simplifications in the C^2 model), Fig. 8 compares the velocities v_{C^2} and v_2 on a representative extract along the time axis. What can be seen is a delay of approximately $0.7\,\mathrm{s}$ between desired input acceleration and the ACC reaction, however for decelerations the delay is only $0.1\,\mathrm{s}$. This asymmetry results in a peak difference of about 3% between desired and achieved velocities, and also to a misalignment between delayed velocities, nearly undelayed steering angles (delay below $0.01\,\mathrm{s}$) and the actual track position. Since both steering wheel angle magnitudes and reaction times match the desired values closely, they are not depicted. This implies that the main source of error between $\boldsymbol{\xi}_1$ and $\boldsymbol{\xi}_2$ are the simple ACC and steering ratio, which are likely outperformed by state-of-the-art drive-by-wire systems.

V. Conclusion

In this paper, the C^2 model was derived geometrically and applied to different maneuvers for different purposes in the simulation tool CarMaker by IPG. It could be shown that the analytic possibilities of this model are adequate. A given trajectory can be analyzed for the internal state parameters of a vehicle with an accuracy of more than 99.9% for velocities and less than 99.7% for steering angles. This may allow for applying the C^2 model for purposes like reconstructing accidents or constraining trajectory optimizations.

A second purpose of the C^2 model was to use the state parameters $a, \bar{\delta}$ (acceleration and mean tire steering angle) as inputs to a drive-by-wire system. Due to the simplicity of the drive-by-wire model, the results merely present a lower bound of quality. Still a deviation of just $3\,\mathrm{cm}/1\,\mathrm{m}$ per driven length was be achieved for a simple open-loop (non-feedback) controller.

The results are promising; however it is necessary to produce a more sophisticated evaluation of the C^2 model. A wider range of maneuvers must be evaluated to assess the analytic potential of the C^2 model; also, real measurements of actual vehicles must be used to complement the simulated data to study the influence of uncertainties. Furthermore, tests with more realistic drive-by-wire systems are necessary to determine the degree of confidence, by which C^2 model outputs can be used as open-loop control inputs to reproduce a trajectory. These tests need to comprise both simulations with more sophisticated models, and tests in actual vehicles equipped with drive-by-wire functionality. A significant increase in quality of the C^2 model predictions is anticipated, however a quantitative estimate is not possible at this stage.

Acknowledgment

This work was partially supported by Valeo Schalter und Sensoren GmbH within the V50 project, and by the Fraunhofer-Gesellschaft along with the state of Baden-Württemberg within their joint innovation cluster REM 2030.

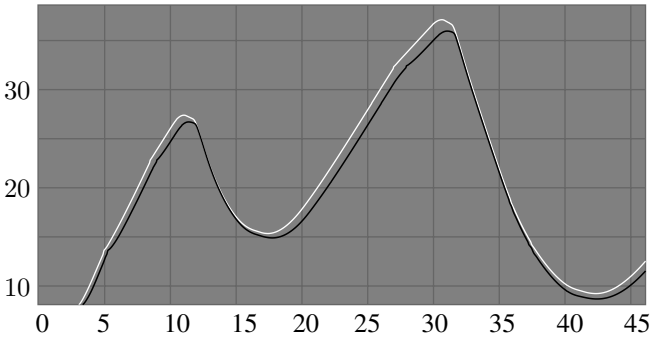

Fig. 8: v_{C^2} (white) and v_2 (black) in $[\mathrm{m/s}]$ over t in $[\mathrm{s}]$, showing the effect of the delay of the drive-by-wire ACC.

References

[1] E. Bauer, F. Lotz, M. Pfromm, M. Schreier, B. Abendroth, S. Cieler, A. Eckert, A. Hohm, S. Lüke, P. Rieth, V. Willert, and J. Adamy. PRORETA 3: An Integrated Approach to Collision Avoidance and Vehicle Automation. *at – Automatisierungstechnik*, 60(12):755–765, 2012.

[2] B. Dubrovin, A. Fomenko, S. Novikov, S. Novikov, and R. Burns. *Modern Geometry - Methods and Applications: Part 3: Introduction to Homology Theory*. Graduate Texts in Mathematics. U.S. Government Printing Office, 1990.

[3] J. Eschenburg and J. Jost. *Differentialgeometrie und Minimalflächen*. Springer London, Limited, 2007.

[4] D. Ferguson, T. M. Howard, and M. Likhachev. Motion Planning in Urban Environments. In M. Buehler, K. Iagnemma, and S. Singh, editors, *The DARPA Urban Challenge*, volume 56, pages 61–90. Springer Berlin Heidelberg, 2009.

[5] R. Isermann. *Fahrdynamik-Regelung: Modellbildung, Fahrerassistenzsysteme, Mechatronik*. Friedr. Vieweg & Sohn Verlag, Wiesbaden, 2006.

[6] M. Montemerlo, J. Becker, S. Bhat, H. Dahlkamp, D. Dolgov, S. Ettinger, D. Haehnel, T. Hilden, G. Hoffmann, B. Huhnke, D. Johnston, S. Klumpp, D. Langer, A. Levandowski, J. Levinson, J. Marcil, D. Orenstein, J. Paefgen, I. Penny, A. Petrovskaya, M. Pflueger, G. Stanek, D. Stavens, A. Vogt, and S. Thrun. Junior: The Stanford Entry in the Urban Challenge. In M. Buehler, K. Iagnemma, and S. Singh, editors, *The DARPA Urban Challenge*, volume 56, pages 91–124. Springer Berlin Heidelberg, Berlin and Heidelberg, 2009.

[7] S. Schmidt and R. Kasper. Ein hierarchischer Ansatz zur optimalen Bahnplanung und Bahnregelung für ein autonomes Fahrzeug. *at – Automatisierungstechnik*, 60(12):743–754, 2012.

[8] D. Schramm, M. Hiller, and R. Bardini. *Modellbildung und Simulation der Dynamik von Kraftfahrzeugen*. Springer Berlin Heidelberg, Berlin and Heidelberg, 2010.

[9] D. J. Struik. *Lectures on Classical Differential Geometry*. Dover Publications, 2nd edition, 1961.

[10] B. Van Brunt. *The Calculus of Variations*. Springer, 2010.

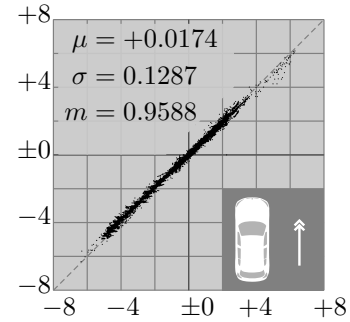

(a) $a_1 \mapsto a_{C^2}$, [m/s^2]

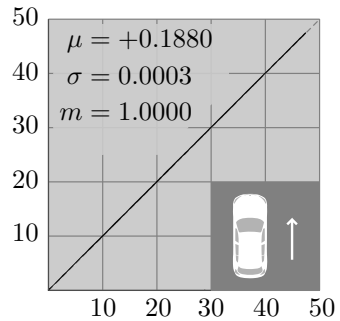

(b) $v_1 \mapsto v_{C^2}$, [m/s]

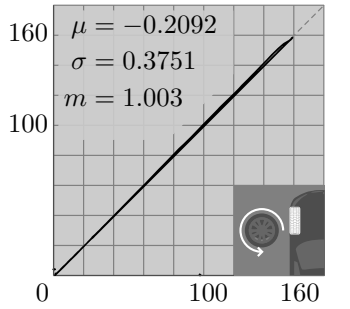

(c) $\dot{\rho}_1^{\text{fl}} \mapsto \dot{\rho}_{C^2}^{\text{fl}}$, [rad/s]

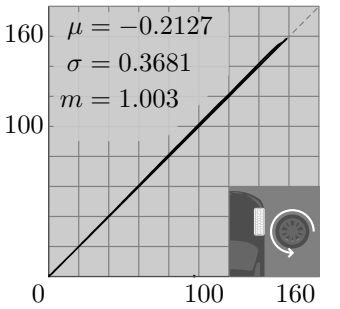

(d) $\dot{\rho}_1^{\text{fr}} \mapsto \dot{\rho}_{C^2}^{\text{fr}}$, [rad/s]

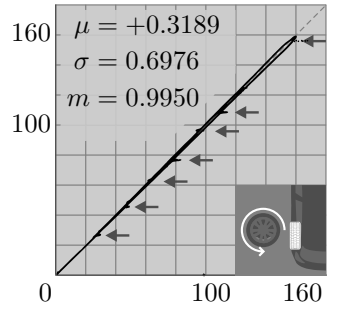

(e) $\dot{\rho}_1^{\text{rl}} \mapsto \dot{\rho}_{C^2}^{\text{rl}}$, [rad/s]

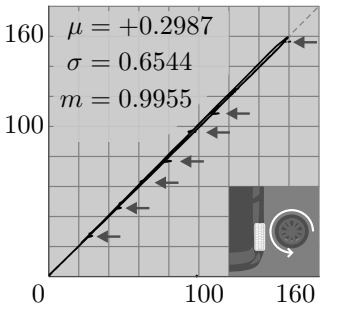

(f) $\dot{\rho}_1^{\text{rr}} \mapsto \dot{\rho}_{C^2}^{\text{rr}}$, [rad/s]

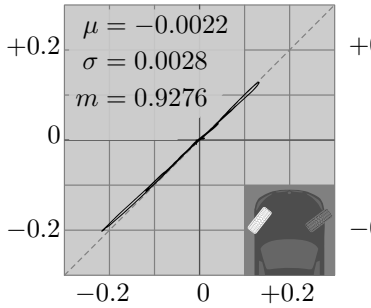

(g) $\delta_1^{\text{left}} \mapsto \delta_{C^2}^{\text{left}}$, [rad]

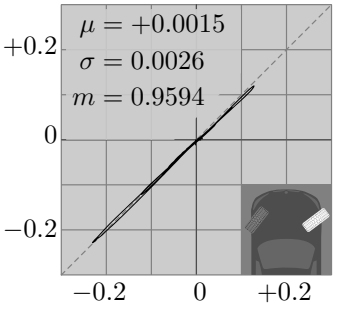

(h) $\delta_1^{\text{right}} \mapsto \delta_{C^2}^{\text{right}}$, [rad]

Fig. 9: Correlation plots of the vehicle parameters along the Hockenheimring track. The vertical axis always refers to the C^2 model estimates, the horizontal axis shows the true data. Mean error μ and standard deviation σ are given inside the plots along with the slope m of the least squares linear approximation, to indicate systematic scale errors. (a): Acceleration. (b): Velocity. (c)–(f): Rotation speeds for each of the wheels. The arrows in (e) and (f) indicate errors due to longitudinal slip when either brake (peak to the left) or gas pedal (peak to the right) are pushed notably. (g), (h): Steering angles for the front wheels.

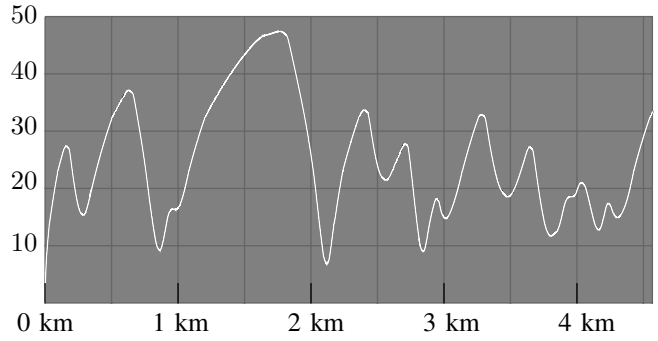

(a) $v = \langle \dot{\boldsymbol{\xi}} | \boldsymbol{T} \rangle$ in [m/s]

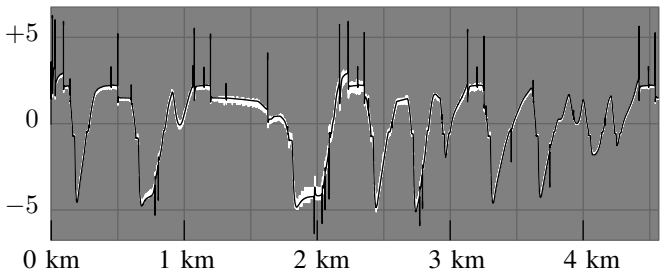

(b) a in [m/s^2]

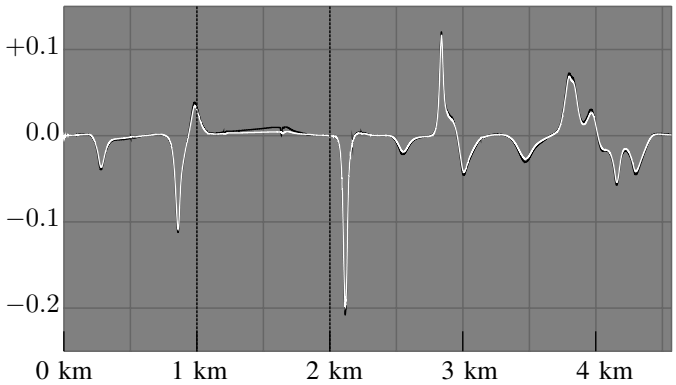

(c) δ in [rad]

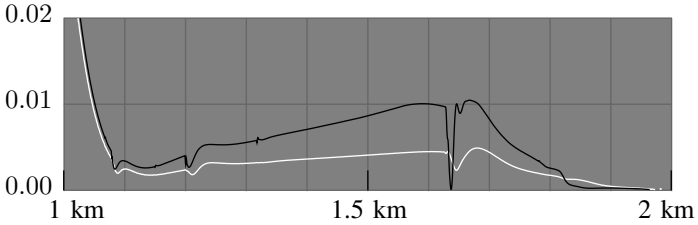

(d) δ in [rad]

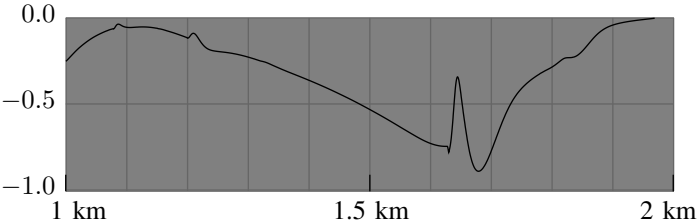

(e) $\langle \dot{\boldsymbol{\xi}} | \boldsymbol{N} \rangle$ in [m/s]

Fig. 10: Parameters extracted along the Hockenheimring (white) compared to true simulation data (black). (d) and (e) show the effect of oversteering that is not modeled, leading to underestimated steering angles during slip. The C^2 model estimate in (e) is zero, since slip is not modeled.